Princeton Plasma Physics Laboratory

PPPL- 5067

PPPL-5067

A New Spectrometer Design for the X-ray Spectroscopy of Laser-produced Plasmas with High (sub-ns) Time Resolution

M. Bitter, K. W. Hill, P. C. Efthimion, L. Delgado-Aparicio,
N. Pablant, Jian Lu, P. Beiersdorfer, and Hui Chen

SEPTEMBER 2014

PPPL PRINCETON PLASMA PHYSICS LABORATORY

Prepared for the U.S. Department of Energy under Contract DE-AC02-09CH11466.

Princeton Plasma Physics Laboratory
Report Disclaimers

Full Legal Disclaimer

Trademark Disclaimer

PPPL Report Availability

Princeton Plasma Physics Laboratory:

http://www.pppl.gov/techreports.cfm

Office of Scientific and Technical Information (OSTI):

http://www.osti.gov/scitech/

Related Links:

U.S. Department of Energy

Office of Scientific and Technical Information

A new spectrometer design for the x-ray spectroscopy of laser-produced plasmas with high (sub-ns) time resolution[a)]

M. Bitter,[1,b)] K. W. Hill,[1] P. C. Efthimion,[1] L. Delgado-Aparicio,[1] N. Pablant,[1] Jian Lu,[2] P. Beiersdorfer,[3] and Hui Chen[3]
[1]*Princeton Plasma Physics Laboratory, Princeton, New Jersey 08543, USA*
[2]*Department of Engineering, Chongqing University, Chongqing 400044, China*
[3]*Physics Division, Lawrence Livermore National Laboratory, Livermore, California 94550, USA*

(Presented 4 June 2014; received 1 June 2014; accepted 17 August 2014; published online 12 September 2014)

This paper describes a new type of x-ray crystal spectrometer, which can be used in combination with gated x-ray detectors to obtain spectra from laser-produced plasmas with a high (sub-ns) time resolution. The spectrometer consists of a convex, spherically bent crystal, which images individual spectral lines as perfectly straight lines across multiple, sequentially gated, strip detectors. Since the Bragg-reflected rays are divergent, the distance between detector and crystal is arbitrary, so that this distance can be appropriately chosen to optimize the experimental arrangement with respect to the detector parameters. The spectrometer concept was verified in proof-of-principle experiments by imaging the Lβ_1- and Lβ_2-lines of tungsten, at 9.6735 and 9.96150 keV, from a micro-focus x-ray tube with a tungsten target onto a two-dimensional pixilated Pilatus detector, using a convex, spherically bent Si-422 crystal with a radius of curvature of 500 mm. © *2014 AIP Publishing LLC*. [http://dx.doi.org/10.1063/1.4894390]

I. INTRODUCTION

The studies of matter under extreme conditions at high-power laser facilities and coherent light sources require x-ray spectroscopic measurements of the plasma density and ion and electron temperatures with very high, sub-ns, time resolutions. An often used technique is the backlighting technique,[1] where the plasma is irradiated by a short burst of high-energy x-rays, which are emitted from a second laser target, e.g., a metal foil, and where the radiation that is scattered or absorbed by the plasma is analyzed with an x-ray crystal spectrometer. In Ref. 1, a toroidally bent Ge-220 crystal was used in combination with a CCD detector. This spectrometer also provided a one-dimensional spatial resolution perpendicular to the main diffraction plane. Toroidally bent crystals can be designed to eliminate the astigmatism for one particular wavelength, but they are not free of image distortions. A von Hamos-like spectrometer with a spherically bent crystal, which has a higher degree of symmetry, may be used in the future to avoid such image distortions.[2] A limitation of the backlighting method is that only one time frame is obtained from an experiment and that many reproducible experiments are needed to document the full time history of the plasma.

A method, which provides several time frames per ns and which thereby facilitates a study of the plasma's time evolution in a single experiment, makes use of gated Multi-Channel-Plate (MCP) detectors to record x-ray emission spectra of highly charged ions from high-Z elements that are added to the laser target as dopant.[3–10] This technique was efficiently used by Glenzer *et al.* at the Nova laser facility. In these experiments, the radiation emitted from the plasma was observed with use of a crystal spectrometer through a crossed slit configuration of one vertical and four horizontal slits, and the spectra were recorded on the four strips of a MCP detector. The horizontal slits provided spatial resolution in the vertical dimension. Since the gate pulse traversed a strip in 250 ps and since the strips were gated sequentially in time intervals of 250 ps, four spectra were obtained in 1 ns. The crystals used were, however, flat crystals or cylindrically bent crystals, which are not optimal with regard to image distortions.

In this paper, we describe a new type of spectrometer, which makes use of the symmetry properties of a convex spherically bent crystal to avoid image distortions and which – in combination with a gated x-ray detector – should provide sub-ns time resolution as well as high spectral resolution. The spectrometer concept is described in Sec. II A, and the results from laboratory x-ray tests, which verified the spectrometer concept, are reported in Sec. II B.

II. SPECTROMETER

A. Spectrometer concept

The working principle of this new spectrometer is illustrated in Fig. 1, which shows a convex spherically bent crystal with a certain radius of curvature R and the ray pattern for a Bragg angle $\Theta = 35^\circ$ that was arbitrarily chosen. Also shown is a circle with the radius RT = R cos (Θ) about the center M of the crystal sphere. The incident and reflected rays are tangential to this circle when the Bragg condition is satisfied for the Bragg angle Θ. The working principle is readily understood if one first considers the imaging of a point source by a concave spherical crystal, assuming that this point source

[a)]Contributed paper, published as part of the Proceedings of the 20th Topical Conference on High-Temperature Plasma Diagnostics, Atlanta, Georgia, USA, June 2014.

[b)]Author to whom correspondence should be addressed. Electronic mail: bitter@pppl.gov

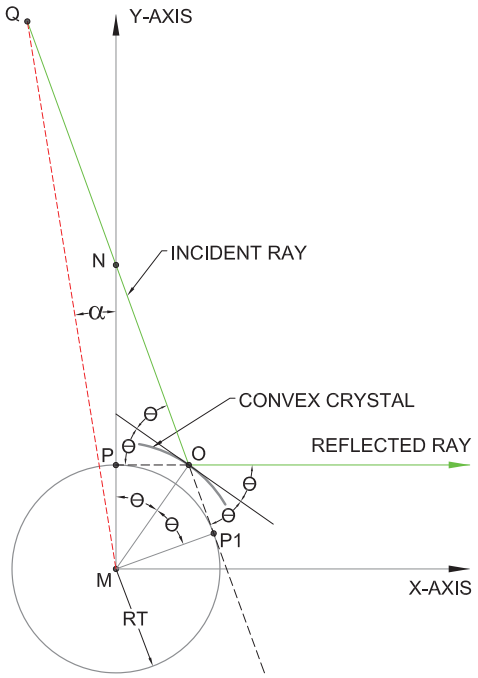

FIG. 1. Illustration of the spectrometer concept, which is further explained in the text.

is at the point P, at the distance u = R sin (Θ) from the central point O on the crystal surface. For a Bragg angle Θ = 35° – and, in general, for Bragg angles Θ < 45° – this distance u is shorter than the focal length f_s = R/[2 sin(Θ)] for the sagittal rays, so that according to Coddington's equations[11] the image produced by the sagittal rays of the point source at P is a virtual image located at the point N, as shown in Fig. 1. In other words, the sagittal rays emitted from a point source at P are divergent after reflection from a concave spherical crystal and seem to originate from a virtual point source at N. If we now replace the concave spherical crystal by a convex spherical crystal and put a real point source at N, where the virtual image was, then the virtual image will be at P, where the source was, so that the reflected ray seems to originate from a virtual point source at P. Since the ray pattern is symmetric with respect to a rotation about the axis MN, it is also clear that the reflected rays, which seem to emanate from the virtual point source at P, are divergent and propagate in a plane that is normal to MN. Therefore, the reflected rays intersect a detector plane, which is perpendicular to the drawing plane and to the ray PO, in a perfectly straight line. If the detector is a gated strip detector, one would orient the detector such that the strips of the detector are either parallel or perpendicular to this line of intersection. Since the reflected rays are divergent, the detector can be placed at an arbitrary distance from the crystal. This distance can therefore be appropriately chosen to optimize the experimental arrangement with regard to the detector parameters.

In addition to the configuration, which was described above, other configurations of the source and its virtual image are possible for the same Bragg angle Θ. In fact, the source can be moved to an arbitrary point Q on the line ON without changing the Bragg angle. The virtual image, from which the reflected rays then seem to emanate, would be at a point P′, at the intersection of the extended line PO with the line MQ. The ray pattern would then be symmetric with respect to a rotation about the new optical axis MQ, and the reflected rays would be on the surface of a cone about the axis MQ. The curve of intersection of this cone with the above mentioned detector plane will not deviate much from a straight line, if the angle α between the line MQ and the y-axis is small.

B. Wavelength dispersion

In this section, we derive the wavelength dispersion relation for an arbitrary experimental arrangement, which is defined if the crystal-source distance $\overline{OQ}$ and the crystal-detector distance are specified. We first analyze the ray pattern for a certain reference spectral line with the Bragg angle $\Theta = \Theta_0$ and an angle $\alpha = \alpha_0$ between the MQ-axis and the y-axis.

For this reference spectral line, we obtain the following equations by an inspection of Fig. 1:

$$\overline{MQ}\sin(2\theta_0 + \alpha_0) = \overline{OQ} + R\sin(\theta_0), \tag{1}$$

$$\overline{MQ}\cos(2\theta_0 + \alpha_0) = R\cos(\theta_0). \tag{2}$$

Since the crystal-source distance $\overline{OQ}$ is given, these equations can be solved for $\overline{MQ}$ and α_0. From Eqs. (1) and (2), we obtain

$$\tan(2\theta_0 + \alpha_0) = \frac{\overline{OQ} + R\sin(\theta_0)}{R\cos(\theta_0)}, \tag{3}$$

which can be solved for α_0. The source distance $\overline{MQ}$ is then obtained from Eq. (2).

The angle α for an arbitrary spectral line with the Bragg angle Θ is then obtained from Eq. (4),

$$\overline{MQ}\cos(2\theta + \alpha) = R\cos(\theta), \tag{4}$$

which is the analogon of Eq. (2).

Knowing the angle α as a function of Θ, we can rotate the ray pattern for each spectral line around M by an angle −α, so that the corresponding MQ-axis coincides with the y-axis. The reflected ray then makes an angle −α with the x-axis and crosses the y-axis at Rcos(Θ)/cos(α). In the x,y-coordinate system with origin at M the equation of the reflected ray is

$$y = \frac{R\cos(\theta)}{\cos(\alpha)} - x\tan(\alpha). \tag{5}$$

This equation can be rewritten as

$$x\sin(\alpha) + y\cos(\alpha) = R\cos(\theta). \tag{6}$$

To derive the wavelength dispersion, we determine the coordinates (x_s, y_s) of the intersection points of the reflected rays with the detector plane, which is assumed to be normal to the reflected ray of the reference spectral line and at a distance Rsin(Θ_0) + d from the origin M of the x,y-coordinate system. The equation of the detector plane is

$$x\cos(\alpha_0) - y\sin(\alpha_0) = R\sin(\theta_0) + d. \tag{7}$$

We note that, before a common rotation of the radiation pattern and the detector plane about M by an angle $-\alpha_0$, the

detector plane would be parallel to the y-axis and at a distance $R\sin(\Theta_0) + d$ from the points P and M. After this rotation, the distance of the detector plane from the point M is still equal to $R\sin(\Theta_0) + d$, as shown on the RHS of Eq. (7), since this distance is not changed by a rotation about M. The coordinates (x_s, y_s) of the intersection points of the reflected rays with the detector plane are the solutions of Eqs. (6) and (7). The wavelength dispersion on the detector is then given by Eq. (8),

$$\xi = \sqrt{(x_s - x_s^0)^2 + (y_s - y_s^0)^2}, \tag{8}$$

where ξ is the distance of the intersection point (x_s, y_s), which is associated with a spectral line of a wavelength λ and Bragg angle Θ, from the intersection point (x_s^0, y_s^0), which is associated with the reference spectral line of the wavelength λ_0 and Bragg angle Θ_0.

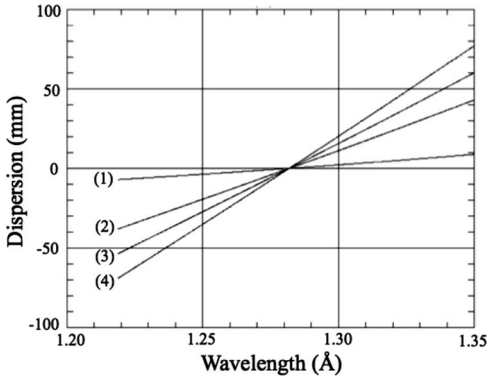

FIG. 3. Calculated wavelength dispersion as explained in the text. The curves (1) through (4) represent the dispersion relations for the crystal-detector distances of d = 0, 508, 762, and 1016 mm, respectively. The dispersion relation for d = 0 is used to determine the area of the crystal, which is irradiated by the source. The effective area of the crystal must be known to calculate the photon throughput.

III. EXPERIMENTAL TESTS

The spectrometer concept was tested by imaging the Lβ_1- and Lβ_2-lines of tungsten, at 9.67235 and 9.96150 keV, from a micro-focus x-ray tube[12] with a tungsten target (x-ray focus size 13 μm) onto a two-dimensional pixilated detector, using a convex, spherically bent Si-422 crystal with a 2d-spacing of 2.21707 Å. The Si-422 crystal had a radius of curvature of 500 mm and an area of 75 × 15 mm^2. The detector was a 100 K Pilatus detector[13] with 487 × 194 pixels of a pixel size of 172 μm and a sensitive area of 83.3 × 33.3 mm^2. Spectra of the tungsten Lβ_1- and Lβ_2-lines were recorded for crystal-detector distances of d = 0, 508, 762, and 1016 mm. The crystal-source distance was fixed at 914.4 mm.

Shown in Fig. 2(a) are the raw spectral data obtained for a crystal-detector distance of d = 1016 mm. As expected, the spectral features appear as straight lines on the detector. Figure 2(b) is a lineout of the spectral data from Fig. 2(a), which represents the sum of the photon counts along the vertical direction on the detector. The peak positions of the Lβ_1-line and Lβ_2-line, with the theoretical wavelengths of λ = 1.28184 Å and λ = 1.24463 Å, were determined from least-squares fits of single Lorentzians to the experimental data, shown in Fig. 2(b), yielding the pixel numbers of 153.448 and 391.551, respectively. Thus, these peaks were separated by 235.103 pixels or 40.44 mm. The latter value deviates by 0.50 mm from the value of 40.94 mm predicted by the dispersion relation for a crystal-detector distance of d = 1016 mm, see Fig. 3. This deviation is within the experimental error of our alignment of the x-ray source, crystal, and detector. The dispersion relations, shown in Fig. 3, were calculated from Eqs. (1) through (8) for a fixed crystal-source distance of 914.4 mm and varying crystal-detector distances, choosing the Lβ_1-line as reference line.

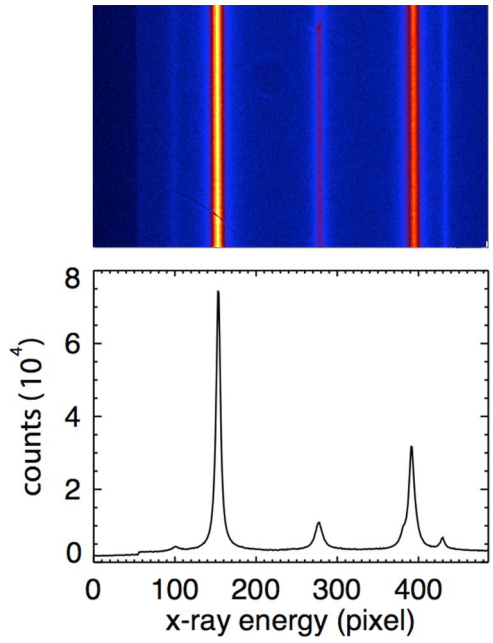

FIG. 2. (a) Raw spectral data recorded by a Pilatus detector. (b) Total number of photon counts, obtained by summing the photon counts along the entire height of the detector, vs pixel number.

The $_{74}$W L emission spectra and satellites were thoroughly investigated in Ref. 14, where the observed line shapes were evaluated by single Lorentzian fits, multiple Lorentzian fits, and even by fits of Voigt functions to extract the natural line widths. The widths of the Lβ_1-line and Lβ_2-line that were obtained from single Lorentzian fits and reported in Ref. 14 were 6.76 eV and 10.39 eV, respectively. Earlier line width measurements of the Lβ_1- and Lβ_2-lines by Salem *et al.*[15] gave values of 7.82 ± 0.63 eV and 9.26 ± 9.3 eV, respectively.

It is of interest to compare these results with our own line width measurements to properly assess the capabilities of our spectrometer. Figure 4 shows again the spectral data from Fig. 2(b) as a function of x-ray energy and the least-squares fits of single Lorentzians to the observed Lβ_1- and Lβ_2-line profiles. The full widths at half maximum of these single Lorentzian fits to the Lβ_1- and Lβ_2-lines were 7.49 eV and 10.6 eV, respectively. These values are in excellent agreement with those reported in Refs. 14 and 15. This result is remarkable, since no corrections were made for the source size broadening, the finite width of the crystal's rocking curve, and a potential line broadening due to the curvature of the spectral

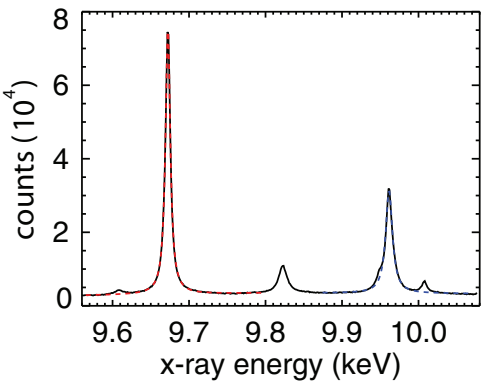

FIG. 4. Spectral data as a function of x-ray energy and least squares fits of Lorentzians to the observed Lβ_1- and Lβ_2-profiles at the energies of 9.67235 and 9.96150 keV. The small hump on the left wing of the Lβ_2-profile is due to the Lβ_{15} line, see also Fig. 2 and Table I in Ref. 14.

lines on the detector. These instrumental effects are discussed in more detail below.

An estimate of the source size broadening can be obtained by considering the emission of photons of, e.g., the Lβ_1-line with the wavelength $\lambda = 1.28184$ Å, from the edge points of the 13 μm wide micro focus of our x-ray tube. These photons are imaged to two detector points, which are about 14 μm apart, as can be shown by performing small rotations of the ray pattern about M that move the source point by ± 6.5 μm. Photons of the same wavelength, $\lambda = 1.28184$ Å, are thereby spread over a 14 μ long detector segment. On the other hand, according to the dispersion relation for d = 1016 mm, see Fig. 3, a 14 μm long detector segment corresponds to a wavelength difference of $\Delta\lambda = 1.2 \times 10^{-5}$ Å or a difference in x-ray energy of $\Delta E = 0.1$ eV. The uncertainty of the x-ray energy, which results from source size broadening, is therefore $\Delta E = 0.1$ eV. The width of the rocking curve of the Si-422 crystal for Bragg reflection of Lβ_1-photons is $\Delta\Theta = 12$ μrad. Inserting this value for $\Delta\Theta$ into the formula $\Delta E/E = \Delta\Theta/\tan(\Theta)$, one finds that $\Delta E = 0.17$ eV. This value of ΔE represents the additional broadening of the observed spectral line, if the crystal's rocking curve can be approximated by a Lorentzian, since the width of a profile, which is produced by the convolution of two Lorentzians – in this case, the Lorentzian of the crystal rocking curve and the "true" Lorentzian of the Lβ_1-line – is equal to the sum of the widths of the two Lorentzians. The line broadening, which results from a curvature of the spectral lines on the detector can, in principle, be analyzed by dividing the detector in small horizontal segments and evaluating the spectral data in each of those segments separately. The spectrum, which was analyzed here and which is shown in Fig. 2(b) and in Fig. 4, was, however, obtained by summing the photon counts along the total height of the detector.

IV. CONCLUSIONS

We described a new x-ray crystal spectrometer, which makes use of a convex spherically bent crystal and which – in combination with gated strip detector – should be well suited for measurements of the plasma density and the ion and electron temperatures in laser-produced plasmas with a high (sub-ns) time resolution. This spectrometer is easy to align because of the symmetry of a spherically bent crystal; and since the reflected rays are divergent, the detector can be placed at an arbitrary distance from the crystal, so that it is possible to optimize the experimental arrangement with respect to the detector parameters. The spectrometer concept was verified by measuring the $_{74}$W L emission spectrum, using a micro focus x-ray tube with a tungsten target. The observed and the theoretically predicted wavelength dispersions on the detector were in agreement within the experimental error. The widths of the W Lβ_1-line and W Lβ_2-line were determined from least-squares fits of single Lorentzians to the experimental data. The results obtained were in excellent agreement with those obtained from the high-precision line width measurements,[13,14] indicating that this new spectrometer is also well suited for line-shape measurements.

ACKNOWLEDGMENTS

This work was supported by the U.S. Department of Energy through Contract Nos. DE-AC02-09CH-11466 and DE-AC52-07NA-27344.

[1]E. J. Gamboa, C. M. Huntington, M. R. Trantham *et al.*, Rev. Sci. Instrum. **83**, 10E108 (2012).
[2]K. W. Hill, M. Bitter *et al.*, Rev. Sci. Instrum. **85**, 11D612 (2014).
[3]C. A. Back, R. L. Kauffman, P. M. Bell, and J. D. Kilkenny, Rev. Sci. Instrum. **66**, 764 (1995).
[4]S. H. Glenzer, C. A. Back, K. G. Estabrook *et al.*, Phys. Rev. E **55**, 927 (1997).
[5]F. J. Marshall and J. A. Oertel, Rev. Sci. Instrum. **68**, 735 (1997).
[6]S. H. Glenzer, G. Gregori, R. W. Lee *et al.*, Phys. Rev. Lett. **90**, 175002 (2003).
[7]J. A. Oertel, R. Aragonez, T. Archuleta *et al.*, Rev. Sci. Instrum. **77**, 10E308 (2006).
[8]S. H. Glenzer, O. L. Landen, P. Neumayer *et al.*, Phys. Rev. Lett. **98**, 065002 (2007).
[9]G. Gregori, S. H. Glenzer, K. B. Fournier *et al.*, Phys. Rev. Lett. **101**, 045003 (2008).
[10]L. R. Benedetti, P. M. Bell, D. K. Bradley *et al.*, Rev. Sci. Instrum. **83**, 10E135 (2012).
[11]G. S. Monk, *Light-Principles and Experiments*, 1st ed. (McGraw-Hill, New York, 1937), p. 52.
[12]Model L9421, Hamamatsu Corporation, Bridgewater, NJ.
[13]Ch. Breonnimann *et al.*, J. Synchrotron Radiation **13**, 120 (2006); see https://www.dectris.com/.
[14]A.-M. Vlaicu, T. Tochio, T. Ishizuka *et al.*, Phys. Rev. A **58**, 3544 (1998).
[15]S. I. Salem, S. L. Panossian, and R. A. Krause, Atomic Data Nucl. Data Tables **14**, 91 (1974).

Princeton Plasma Physics Laboratory
Office of Reports and Publications

Managed by
Princeton University

under contract with the
U.S. Department of Energy
(DE-AC02-09CH11466)

P.O. Box 451, Princeton, NJ 08543
Phone: 609-243-2245
Fax: 609-243-2751

E-mail: publications@pppl.gov
Website: http://www.pppl.gov